

Potential sputtering

BY FRIEDRICH AUMAYR AND HANNSPETER WINTER

*Institut für Allgemeine Physik, Technische Universität Wien,
Wiedner Hauptstrasse 8–10, 1040 Vienna, Austria
(aumayr@iap.tuwien.ac.at)*

Published online 25 November 2003

The potential energy stored in multiply charged ions is liberated when the ions recombine during impact on a solid surface. For certain target species this can lead to a novel form of ion-induced sputtering, which, in analogy to the usual kinetic sputtering, has been termed ‘potential sputtering’. This sputtering process is characterized by a strong dependence of the observed sputtering yields on the charge state of the impinging ion and can take place at ion-impact energies well below the kinetic sputtering threshold.

We summarize a series of recent careful experiments in which potential sputtering has been investigated for hyperthermal highly charged ions’ impact on various surfaces (e.g. Au, LiF, NaCl, SiO₂, Al₂O₃ and MgO), present the different models proposed to explain the potential sputtering phenomenon and also discuss possible applications of potential sputtering for nanostructure fabrication.

Keywords: multi-charged-ion–surface interaction;
potential sputtering; hollow atoms; nanostructuring

1. Introduction

The interaction of energetic ions (atoms) with surfaces leads to a variety of emission phenomena (emission of electrons, photons, atoms, ions, clusters) and results in pronounced modification of the surface and near-surface regions (change in composition and structure, defect production, removal of atoms, etc.) (see, for example, Gnaser (1999) and references therein). The technological relevance of low-energy ion–surface interactions in such diverse fields as surface analysis, implantation, sputter cleaning of surfaces, thin film deposition, etc. (Murty 2002), has provided the stimulus for ongoing investigations into the responsible basic mechanisms.

In kinetic sputtering, the decelerated primary projectiles usually transfer (kinetic) energy and momentum to the target atoms, displacing them from their original position and eventually causing their emission into a vacuum (Sigmund 1993). Singly charged ions with kinetic energies typically of some keV mainly interact by means of a few direct collisions with the target atoms (nuclear stopping) (Ziegler *et al.* 1985). For faster ions and especially swift heavy ions (typically MeV per atomic mass unit), the electronic energy loss (electronic stopping) dominates (Schiwietz *et al.* 2001;

One contribution of 11 to a Theme ‘Sputtering: past, present and future. W. R. Grove 150th Anniversary Issue’.

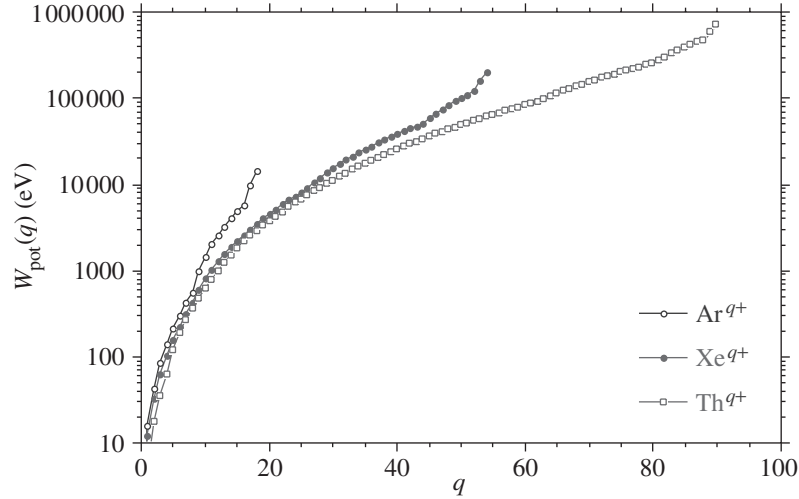


Figure 1. Total potential energy $W_{\text{pot}}(q)$ of multiply charged Ar^{q+} , Xe^{q+} and Th^{q+} ions versus charge state q .

Arnoldbik *et al.* 2003), leading to electronic excitation and ionization in a track a few nanometres in diameter. While the energy dissipation of the fast projectile is well understood, the conversion of electronic excitations into motion of (eventually sputtered) surface atoms is still a matter of debate.

In addition to their kinetic energy, ions can also carry internal (potential) energy, particularly if the ions carry a high charge. In a highly charged ion (HCI), potential energy will be stored according to its production, when q electrons (where q is the ion charge state) have to be removed from an originally neutral atom, and this potential energy becomes rather large for high values of q , as shown in figure 1. Upon surface impact, this potential energy is available for inducing various inelastic processes, while the HCI will regain its q missing electrons to become fully neutralized again (Aumayr 1995; Arnau *et al.* 1997; Winter & Aumayr 1999, 2001, 2002). The HCI deposits its potential energy in a short time (typically *ca.* 100 fs) within a small area (typically less than 1 nm^2). This can lead to strong nonlinear excitation processes, exotic phenomena such as ‘hollow atom’ formation (Arnau *et al.* 1997; Schenkel *et al.* 1999; Winter & Aumayr 1999, 2002) and eventually to the removal of atoms and ions from the target surface (Aumayr *et al.* 1999). Since the energy for the ejection of target atoms and ions results from the potential energy of the ion, this new form of sputtering has been termed ‘potential sputtering’ (PS) (Neidhart *et al.* 1995*b*; Sporn *et al.* 1997; Aumayr *et al.* 1999).

In this paper we will summarize the present knowledge on potential sputtering. To this aim we will present a short history of potential sputtering investigations in § 2 and describe our experimental set-up for measuring total sputter yields and discuss critical experimental issues involved in § 3. Our experimental results are summarized in § 4, while in § 5 we present the different models proposed to explain the PS phenomenon and compare them to experimental results. Finally, in an outlook (§ 6) we discuss possible practical applications of potential sputtering.

2. History of potential sputtering

The first experimental work on charge-state-dependent sputtering of insulators by HCIs was carried out in Tashkent, Uzbekistan (Radzhabov *et al.* 1976; Morozov *et al.* 1979). From this work it was concluded that, for impact of Ar^{q+} ions ($q \leq 5$) on silicon and alkali-halide surfaces, secondary-ion yields increased rapidly both with the incident-ion charge and for decreasing impact energy. Etching patterns on a KCl surface that had previously been bombarded with equal fluxes of slow Ar^{q+} and Kr^{q+} ions were larger for higher q (Radzhabov & Rakhimov 1985). In Eccles *et al.* (1986) it was claimed that, for bombardment of Si with singly charged ions, sputter yields are larger by more than a factor of two than for neutral projectiles of equal mass and energy. However, for 20 keV Ar^{q+} ($q \leq 9$) impact on an Si surface, only the secondary-ion yield increased noticeably with q , whereas the respective total sputter yields (dominated by ejection of neutral Si atoms) did not change with q (de Zwart *et al.* 1986). This apparent contradiction to Eccles *et al.* (1986) was explained by a different conductance of the Si samples.

Atomic force microscopy (AFM) on mica samples irradiated with low fluences of very highly charged ions (e.g. Xe^{44+} and U^{70+}) revealed single-ion-induced blister-like defects, the size of which increased with the incident-ion charge beyond a certain charge-state ‘threshold’ at around $q = 30$ (Schneider *et al.* 1993). These measurements have been performed at comparably high impact energies (several hundred keV), but were repeated later at somewhat lower kinetic energies (100 keV) (Parks *et al.* 1998) with the same results. For bombardment of SiO_2 with Xe^{q+} ($q \leq 44$) and Th^{q+} ($q \leq 70$) at similar kinetic energies as in Schneider *et al.* (1993), time-of-flight (TOF) spectra of ejected positive and negative secondary ions were dominated by single-atomic species, but also molecular clusters could be observed (Schneider & Briere 1996). Again, the yields increased in proportion to the incident-ion charge above a ‘threshold’ of about $q = 25$. Secondary-ion yields were made absolute by taking into account the acceptance solid angle and efficiency of the applied TOF system, resulting in, for example, total yields of 25 ± 12 for positive and 5 ± 2.5 for negative secondary ions, respectively, from impact of Th^{70+} . These remarkably high values suggested that the total sputtering yields (i.e. including neutrals) must be significantly larger than the known kinetic sputtering yield of about 2.5 target particles for impact of 500 keV singly charged Th ions (Schneider & Briere 1996). Further work performed under similar conditions, but using a catcher-foil technique for measuring the total sputtering yield, showed that GaAs and UO_2 surfaces are also much more efficiently ablated by HCIs such as Th^{70+} than is expected from the kinetic projectile energy involved (Schenkel *et al.* 1999).

A different set of results stems from HCI-induced proton sputtering from ‘dirty’ (i.e. untreated, hydrocarbon-covered) surfaces. The proton sputtering yields show a remarkably strong dependence on ion charge q , ranging from $\sim q^3$ in the kinetic sputtering regime (Della-Negra *et al.* 1988; Bitenskii *et al.* 1992) to q^5 – q^6 in the pure potential sputtering regime (Mochiji *et al.* 1994; Kakutani *et al.* 1995b). In addition, a relatively high yield of about one proton per incident highly charged ion ($q = 20$) was measured. An enhancement in secondary-ion emission yield with primary-ion charge state has recently even been claimed for thin ‘conducting’ carbon foils (Schenkel *et al.* 1997). However, the fact that in these experiments almost exclusively hydrocarbon ions, protons and H^- were detected points to sputtering

from an insulating hydrocarbon overlayer rather than sputtering from the conducting amorphous carbon foil.

No firm conclusions can be drawn on the total sputter yield from such secondary-ion-emission measurements. On the other hand, accurate determination of the total sputter yields (including both neutral and ionized secondary particles) has been performed by means of a sensitive quartz-crystal microbalance technique (see §3) developed at Technische Universität (TU) Wien (Neidhart *et al.* 1994; Hayderer *et al.* 1999b). Measurements have been carried out for impact of Ar^{q+} ($q < 14$) and Xe^{q+} ions ($q < 28$) on various surfaces (Neidhart *et al.* 1995b; Sporn *et al.* 1997; Hayderer *et al.* 2001b). For conducting surfaces, no q -dependent total sputter yield (only kinetic sputtering) was observed (Varga *et al.* 1997; Hayderer *et al.* 2001a), while, for alkali halide and some other insulating surfaces, a sizeable sputtering yield could be observed down to very low impact energies (at least $5q$ eV) (Neidhart *et al.* 1995b; Sporn *et al.* 1997; Hayderer *et al.* 2001b), which increased dramatically with the potential energy carried by the projectile, leading to neutral sputtering yields as high as several hundred target particles per single ion impact (respective details are given in §4).

3. The quartz-crystal microbalance technique

To measure total sputter yields (including both neutral and ionized secondary particles) in HCl–surface collisions, a sensitive quartz-crystal microbalance technique has been developed at TU Wien (Hayderer *et al.* 1999b). Whereas quartz crystals are widely used for determination of the area mass and hence the thickness of deposited material, the rate for material removal has mainly been studied by other techniques, such as the conventional microbalance and catcher foils analysed by Rutherford back scattering. This is not astonishing because the use of quartz crystals for sputter-yield measurements encounters severe problems. The rates of material removal, and hence the frequency changes, are rather low compared with most deposition applications, requiring high-frequency stability of the crystal and of the oscillator circuit, as well as high accuracy and resolution of the frequency measurement. Furthermore, a substantial amount of energy is deposited by the primary particles onto the sputtered surface, causing problems due to thermal drift. In many deposition applications, the energy deposition per incident atom is only a few eV (sublimation energy plus heat radiation from the evaporation source), while in our case the energy deposited per sputtered atom is up to a few hundred eV. Other problems arise from the sensitivity of the resonance frequency on surface stress induced by non-uniform mass removal across the ion-beam cross-section.

McKeown (1961) was among the first to use a quartz-crystal microbalance for sputtering measurements (100 eV Ar^+ on Au), and later Ellegard *et al.* (1986) studied electronic sputtering of condensed rare gases with a similar method.

We have improved this technique so that now mass changes as low as 5×10^{-3} monolayers per minute for thin target films can be detected. In our set-up (figure 2) a planoconvex stress-compensated (SC)-cut quartz crystal is first coated with evaporated gold electrodes on a thin chromium adhesion layer. For the measurements with LiF and NaCl, a thin polycrystalline film with a thickness of *ca.* 100 nm was evaporated from an Mo boat onto the front electrode, whereas the measurements on Au were performed by sputtering the quartz Au contact electrodes directly. Deposition

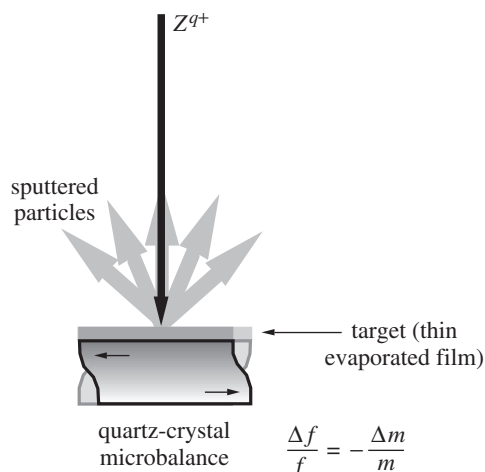


Figure 2. Schematic of a quartz-crystal microbalance technique (see text).

of these electrodes and the formation with LiF and NaCl thin films on the quartz-crystal faces was done in a separate high-vacuum coating system (10^{-6} mbar) at a substrate temperature of *ca.* 150 °C, with deposition rates of the order of 1 nm s^{-1} . For measurements on Si and SiO₂, a pure Cr electrode was used to avoid the formation of Au silicide. Si was deposited *in situ* from an electron-beam (e-beam) heated crucible, whereas GaAs was deposited in a metal-beam-epitaxy system and transported in air to the ultra-high vacuum (UHV) set-up. SiO₂, Al₂O₃ and MgO_x layers have been produced *in situ* by e-beam evaporation of suitable powder at an oxygen pressure of 10^{-3} – 10^{-5} mbar.

All targets have been cleaned by sputtering and heating. To check cleanliness, quality and stoichiometry of the thin films (especially for the alkali halides), secondary-ion mass spectroscopy, Auger-electron spectroscopy and, in some cases, X-ray photoelectron spectroscopy (XPS) have been used. Selection of the oscillator quartz crystal (cut, shape, temperature dependence of resonance frequency) is of great importance for achieving the highest possible mass resolution.

Since the deposited film is very thin compared with the quartz crystal, it is sufficient to use the simple equation

$$\frac{\Delta m}{m} = -\frac{\Delta f}{f}, \quad (3.1)$$

which relates the relative mass loss $\Delta m/m$ to the relative change of frequency $\Delta f/f$.

To determine the total sputter yield independent of the HCI's kinetic energy, one has to consider two important facts which can strongly influence the results. The first point concerns the measurement of the primary-ion current. We used a biased Faraday cup to reduce the influence of ion-induced electrons. Secondly, the energy-dependent influence of primary-ion deposition in the first monolayers at low ion dose directly influences the frequency change in the opposite sense of the sputtering effect until steady-state conditions are reached.

For example, for LiF we have ensured that measurements were performed under steady-state conditions at 100 eV Ne⁺ bombardment. After an Ne⁺-ion dose of $1 \times$

10^{16} ions cm^{-2} , which corresponds to the removal of 2 ML, we no longer observe any significant change in the sputtering rate within an accuracy of 10%.

Our technique does not suffer from the problems inherent to the collection of sputtered particles (e.g. incompletely defined collection geometry and/or neutral-particle sticking coefficients), since the total sputter yields can readily be determined from the frequency change for known ion-current density. High stability of the resonance frequency (*ca.* 1 mHz root-mean-squared frequency noise at 6 MHz) was achieved by operating the quartz crystals within ± 0.1 °C of the minimum of their frequency-versus-temperature curve at 150 °C, which means that the target films also had to be kept at this temperature. The influence of thermal stress arising from temperature gradients due to energy deposition by incoming ions has been strongly reduced by using SC-cut crystals for which the resonance frequency is most insensitive to radial stress.

Finally, we would like to recall specific critical experimental issues which can be encountered when studying the interaction of charged particles with insulating targets. In general, influence of the charge state of the projectile (i.e. its potential energy, represented by the total ionization energy of the respective neutral atom) becomes most effective at the lowest impact velocity, where processes due to the kinetic projectile energy will be drastically reduced or absent altogether. A basic requirement for reproducible results which can be compared with available theory is clean and well-characterized surfaces. Additionally, in the case of polycrystalline targets, structural properties cannot be neglected. For both semiconductor surfaces and insulator surfaces, sputtering and annealing, as commonly applied to metal targets, are less effective or even destructive. The extreme sensitivity of oxides to ion bombardment may cause preferential sputtering of oxygen in the near-surface region, which severely modifies surface properties. Another difficulty in such ion-beam experiments is the possible charging-up of the target surface. Both primary ions and ejected electrons give rise to a positively charged surface layer, which will influence not only the effective ion-impact energy but also the energy distribution of the emitted charged particles. Since energy distributions of secondary ions, as well as ejected electrons, show maxima at a few eV only, a target charge-up to only a fraction of a volt can already strongly influence the total yields. Special precautions are needed to overcome such difficulties (e.g. electron flooding, deposition of insulator target material as ultra-thin films on metal substrates, heating of samples up to a temperature where ion conduction becomes sufficiently large, as for the case of alkali halides).

4. Experimental results

With the quartz-crystal-balance method as described in § 3, sputtering measurements have been carried out for impact of various singly and multiply charged ions (kinetic impact energy below 2 keV) on Au (a metal), alkali halides (LiF and NaCl), oxides (SiO_2 , Al_2O_3 , MgO) and semiconductors (Si, GaAs). Experiments with low to intermediate charge-state ions were performed using a 5 GHz electron cyclotron resonance (ECR) ion-source facility at TU Wien. To investigate projectile ions in higher charge states, our set-up was moved to a 14.5 GHz ECR ion source at Hahn-Meitner-Institut (HMI) Berlin (in collaboration with N. Stolterfoht and co-workers).

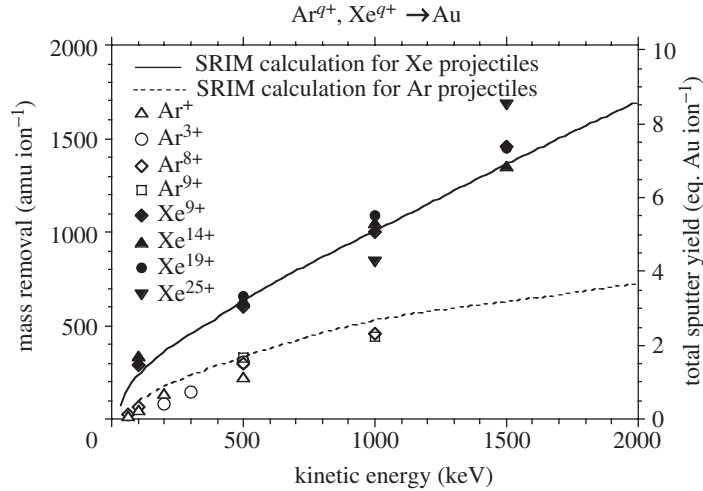


Figure 3. Measured sputter yields of Au for impact of Ar^{q+} (open symbols) and Xe^{q+} ions (full symbols) in various charge states as a function of ion-impact energy. The solid (broken) line shows kinetic sputtering yields as calculated for neutral Xe (Ar) projectiles on Au by the SRIM-2000 code. (Data from Varga *et al.* (1997) and Hayderer *et al.* (2001a).)

(a) Au, Si and GaAs

Dependencies of the measured total sputter yields Y on projectile kinetic energy E_k for HCI impact on the conducting (Au) and semiconducting targets (Si, GaAs) have been plotted in figures 3–5 (using data from Varga *et al.* (1997) and Hayderer *et al.* (2001a)).

Figure 3 shows the mass removal (in atomic mass units per incident ion, as determined by our quartz-crystal microbalance) due to impact of Ar^{q+} ($q = 1, 3, 8, 9$) and Xe^{q+} ($q = 9, 14, 19, 25$) on Au as a function of ion-impact energy. Also shown are kinetic sputtering yields as calculated for neutral Ar and Xe projectiles on Au by the SRIM-2000 code (the most recent version of TRIM (Ziegler *et al.* 1985)). Up to the highest charge states investigated (Xe^{25+}), the sputter yields measured for the Au target remain independent of the projectile charge state. The data points nicely follow the SRIM-2000 results: a code that only considers kinetic sputtering due to momentum transfer in a collision cascade. Therefore, our results provide convincing evidence that, for a conducting Au target, the potential energy of highly charged ions (more than 8 keV in the case of Xe^{25+} compared with less than 1.5 keV kinetic energy of these ions) is not relevant for sputtering of surface atoms.

No significant dependence on projectile charge state (and thus potential energy) was found for our Si- and GaAs-target films (cf. figures 4 and 5). On the contrary, the determined yield data depend on impact energy, as expected only for kinetic sputtering, and exhibit a threshold behaviour at the lowest impact energies.

(b) LiF and NaCl

For alkali-halide target films, the measured total sputter yields dramatically increase with increasing charge state (cf. figure 6 for LiF and figure 7 for NaCl). What is especially noticeable is that for these targets a considerable sputtering yield

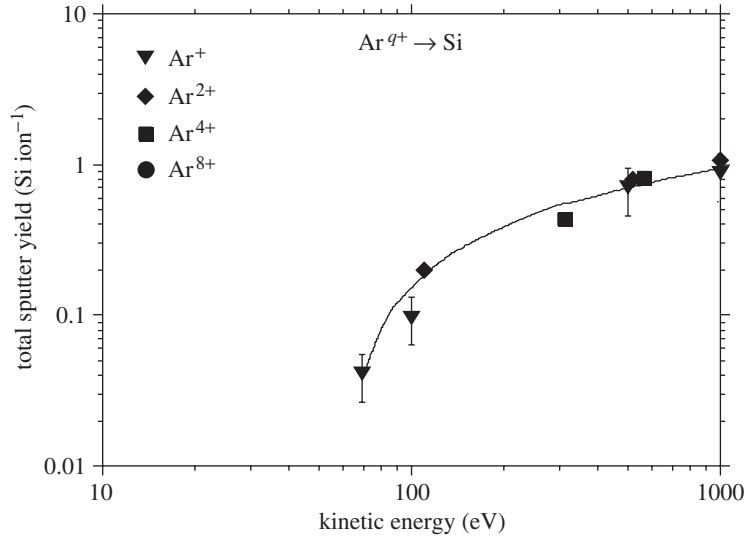


Figure 4. Measured sputter yield of Si for impact of Ar^{q+} ions as a function of ion-impact energy. (Data from Varga *et al.* (1997).)

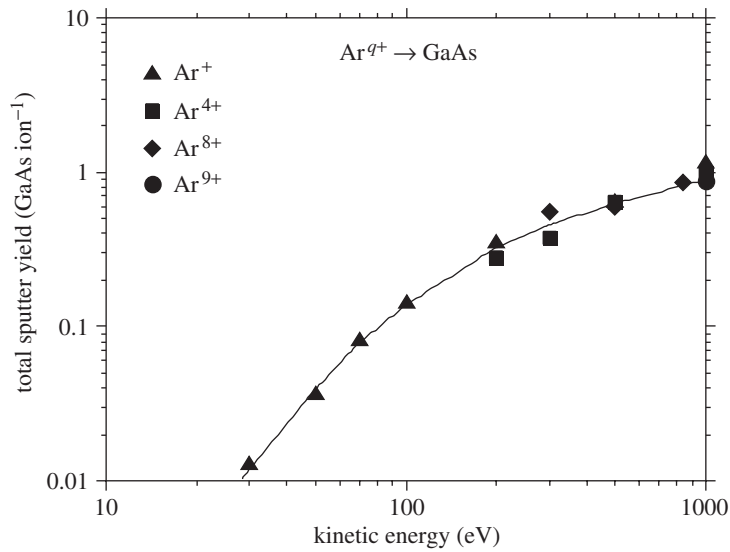


Figure 5. Measured sputter yield of GaAs for impact of Ar^{q+} ions as a function of ion-impact energy. (Data from Varga *et al.* (1997).)

can be observed down to the lowest impact energies accessible in our measurements (typically $5q$ eV) with no apparent impact energy threshold, as in the case of kinetic sputtering.

For a fixed (nominal) impact energy of 100 eV (the actual impact energies will be slightly higher due to image charge attraction—see §5) the dependence of the measured total sputter yields has been plotted as a function of the available potential (recombination) energy of the incident ion in figure 8a. The linear increase in

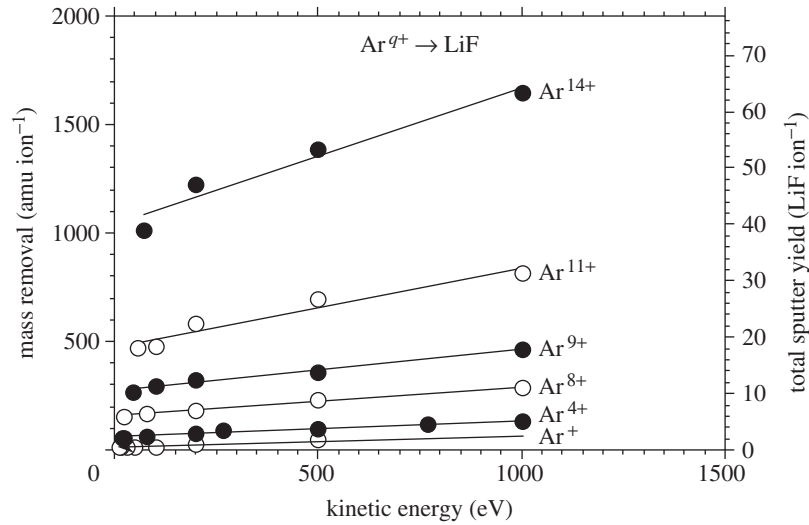


Figure 6. Measured sputter yield of LiF for impact of Ar^{q+} ions as a function of ion-impact energy. (Data from Neidhart *et al.* (1995b) and Sporn *et al.* (1997).)

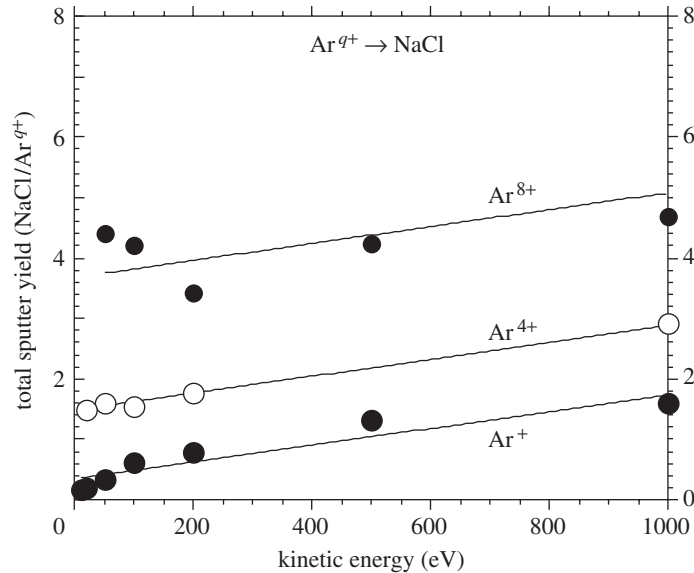


Figure 7. Measured sputter yield of NaCl for impact of Ar^{q+} ions as a function of ion-impact energy. (Data from Varga *et al.* (1997).)

the sputter yield with recombination energy (at fixed kinetic energy) is convincing evidence that the potential energy of the projectile is the source of mass removal from the target film.

In analogy to the impact energy threshold in kinetic sputtering, we have searched for the potential-energy threshold, i.e. the minimum potential energy necessary to induce potential sputtering. To this aim we have determined total sputtering yields for LiF under impact of various singly and doubly charged ions (at 100 eV kinetic

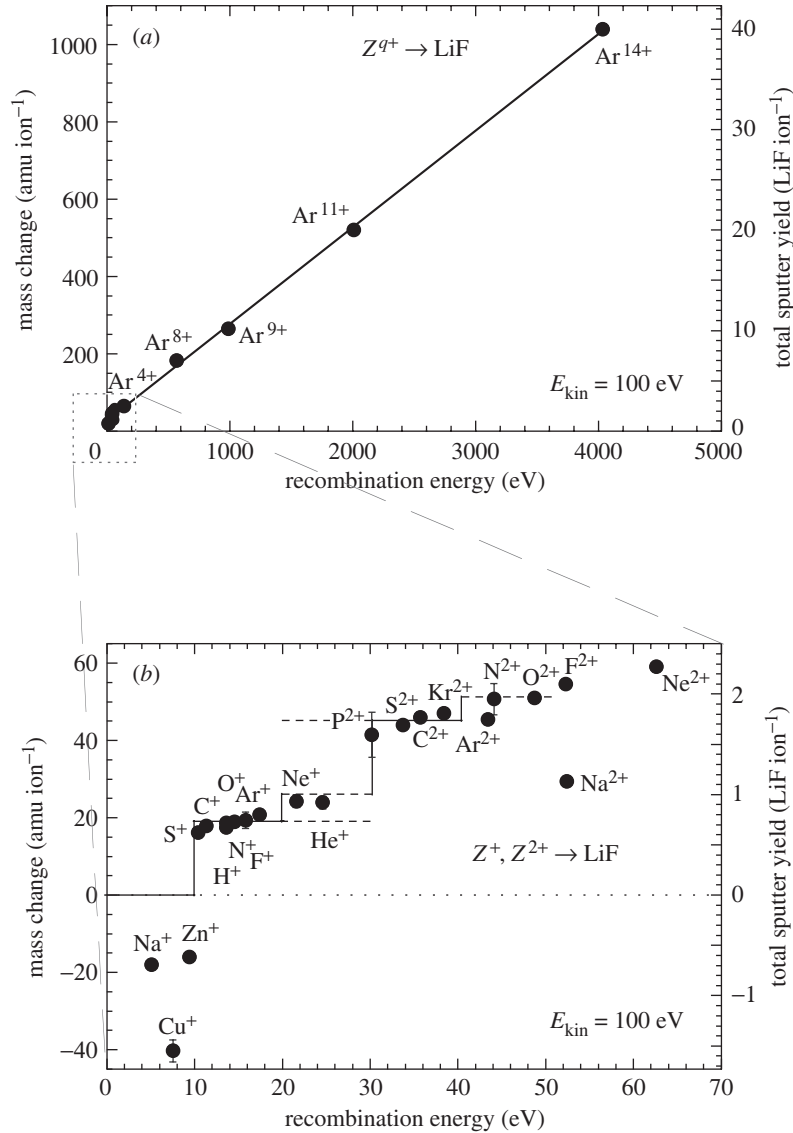


Figure 8. (a) Ion-induced sputtering yield for LiF as a function of the available potential (recombination) energy of the incident ion at a fixed kinetic impact energy of 100 eV. (b) The blow-up of the region around the origin shows that a minimum potential energy of *ca.* 10 eV (threshold) is necessary in order to induce potential sputtering of LiF. (Data from Neidhart *et al.* (1995b), Sporn *et al.* (1997) and Hayderer *et al.* (1999a).)

energy) (Hayderer *et al.* 1999a). Figure 8b shows that for Na⁺, Cu⁺ and Zn⁺ projectiles (all of which carry a potential energy of less than 10 eV) no target mass decrease is observed. Instead, the quartz-crystal microbalance detects a frequency shift corresponding to material deposition on the LiF surface. A clear threshold for potential sputtering between 9.4 eV (Zn⁺) and 10.4 eV (S⁺) is evident. All other projectiles with ionization potentials larger than that of Zn sputter LiF. As will be discussed

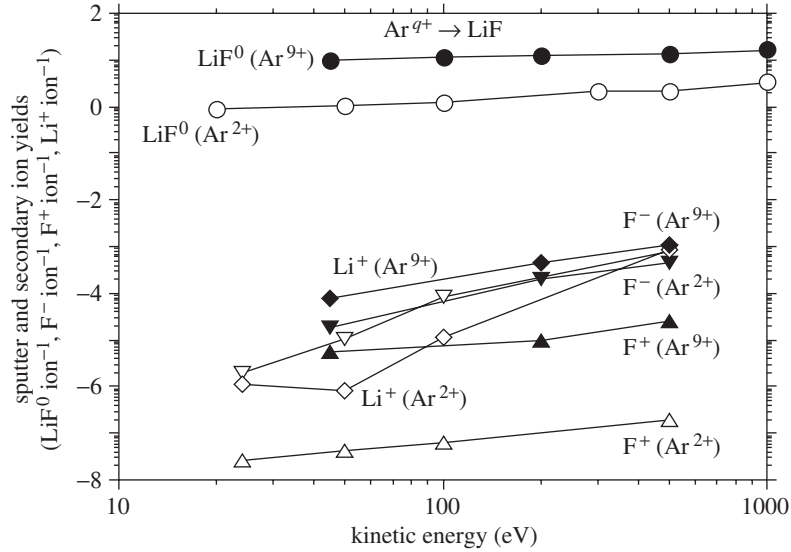


Figure 9. Experimentally determined yields for emission of F^- , F^+ and Li^+ secondary ions due to the impact of Ar^{2+} and Ar^{9+} ions on LiF as a function of ion-impact energy. Total sputter yields are added for comparison. (Data from Neidhart *et al.* (1995c); solid lines are for guidance only.)

in § 5, the measured potential energy threshold of 10 eV gives a strong hint on the responsible sputtering mechanism.

Accompanying secondary-ion yield measurements of F^- , F^+ and Li^+ for LiF showed that the sputter yield is dominated by neutrals (see figure 9) which are at least two orders of magnitude more abundant than secondary ions (Neidhart *et al.* 1995c). Yields of clusters also observed, such as Li^{2+} , LiF^+ , LiF^- , Li_2F^+ and LiF_2^- , are about 2–3 orders of magnitude smaller. This behaviour is probably characteristic for other alkali halides as well.

(c) SiO_2 , Al_2O_3 and MgO_x

The charge-state dependence of sputtering yields was also investigated for oxide targets. Clear signatures of potential sputtering were observed for SiO_2 (figure 10) and Al_2O_3 (figure 11) (Sporn *et al.* 1997; Hayderer *et al.* 2001b). For both targets the measured yields not only strongly increase with charge state but also show a finite sputtering yield when extrapolated to zero impact velocity, as in the case of the alkali halide targets.

A clearly different behaviour was found for MgO (actually MgO_x because XPS measurements showed an oxygen-enriched surface layer) films (figure 12, see also Hayderer *et al.* (2001b)). The sputtering data for this target film show an unusually strong dependence on the ion's kinetic energy. Although the potential energy greatly enhances the total sputtering yield (the yield is also proportional to the potential energy in this case), it does not seem to be sufficient to induce sputtering on its own. Extrapolation of the measured yields to zero-kinetic energy for all charge states is consistent with zero sputtering yield. Only in combination with kinetic energy of the projectile are conspicuously large sputtering yields achieved.

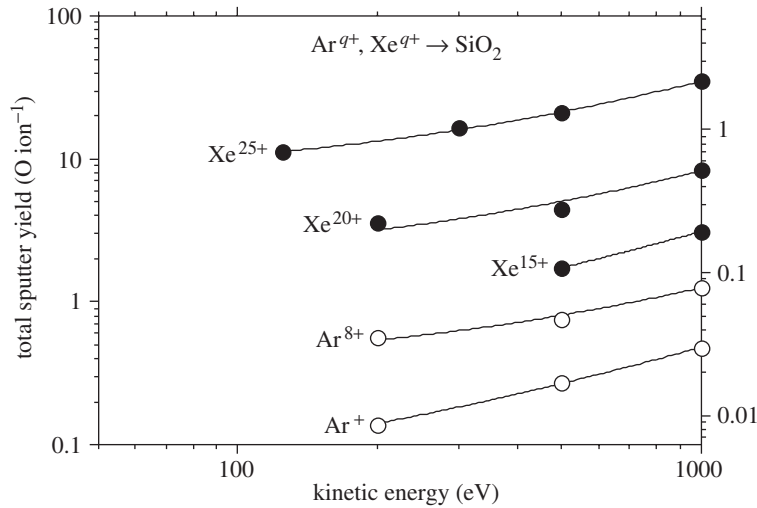


Figure 10. Measured sputter yield of SiO₂ for impact of Ar^{q+} and Xe^{q+} ions as a function of ion-impact energy. (Data from Sporn *et al.* (1997).)

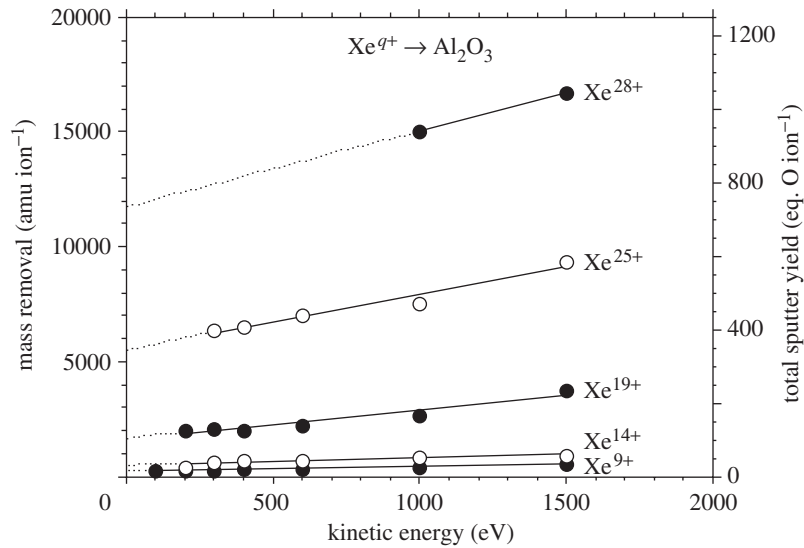


Figure 11. Measured sputter yield of Al₂O₃ for impact of Xe^{q+} ions as a function of ion-impact energy. (Data from Hayderer *et al.* (2001b).)

The data shown in figures 10–12 are values obtained by using freshly prepared surfaces. For all oxides the potential sputtering effect was found to be dose dependent (an example is given in figure 13), i.e. the apparent yield decreased with increasing ion dose, indicating preferential sputtering of oxygen. For example, for 1 keV Xe¹⁴⁺ ions the sputtering yield of Al₂O₃ drastically decreased at an ion dose of 2×10^{13} ions cm⁻² (figure 13) (Hayderer *et al.* 2001a). The integrated mass loss at this total dose corresponds approximately to the removal of all oxygen atoms from the first monolayer (ML) of Al₂O₃. For PS from SiO₂, a surface decomposition due to preferential desorption of oxygen and the formation of an Si overlayer leading

to reduced sputtering has also been demonstrated (Sporn *et al.* 1997; Varga *et al.* 1997).

For the MgO_x target, a much higher ion dose, corresponding to the ablation of *ca.* 10 ML had to be applied before a decrease in sputtering yield became noticeable (Hayderer *et al.* 2001*b*). For all target species, the original sputter values could, however, be restored by re-oxidation of the samples in air. Since post-oxidation of MgO films leads to MgO_2 -enriched surface layers, the observed dose dependence is interpreted as the transition between (a rather thick) oxygen-enriched surface layer and bulk MgO.

In contrast, stoichiometric sputtering has been found for LiF and NaCl surfaces (Neidhart *et al.* 1995*b*; Varga *et al.* 1997).

5. Models for potential sputtering

(a) Interaction of multiply charged ions with surfaces

Slow multi-charged ions interact strongly and selectively with the outermost layers of solid surfaces. Figure 14 illustrates various phenomena that occur during the approach of a slow multi-charged ion in initial charge state q towards a clean metal surface with work function W . A classical over-the-barrier model developed by J. Burgdörfer (see Burgdörfer *et al.* 1991; Burgdörfer 1993) predicts, for $q \gg 1$, the first quasi-resonant electronic transitions from the surface to arise at a ‘critical distance’

$$d_c \approx \frac{(2q)^{1/2}}{W} \quad (5.1)$$

into excited projectile states with hydrogenic principal quantum numbers

$$n_c \approx \frac{q^{3/4}}{W^{1/2}} \text{ (atomic units)}. \quad (5.2)$$

For example, for fully stripped argon ($Z = q = 18$, where Z is the projectile nuclear charge) on Al ($W = 0.16$ atomic units) the classical over-the-barrier model predicts $d_c \approx 2$ nm and $n_c \approx 22$.

The rapid neutralization of the MCI in front of the surface by resonant capture of electrons results in the transient formation of so-called ‘hollow atoms’ or ‘hollow ions’ (cf. Morgenstern & Das 1994; Aumayr 1995; Arnau *et al.* 1997; Hägg *et al.* 1997; Winter & Aumayr 1999, 2002; Winter 2000, and references therein). This hollow atom, an exotic creation from atomic collisions, is a short-lived multiply excited neutral atom which carries the larger part of its Z electrons in high- n levels, while some inner shells remain transiently empty. Such an extreme population inversion can last for typically 100 fs during the approach towards the surface.

Decay of these hollow atoms via auto-ionization and other Auger-type processes is accompanied by the emission of a large number of slow (up to 10 eV) electrons (Aumayr *et al.* 1993). For example, for the impact of a single Th^{80+} ion ($v \approx 10^4$ m s $^{-1}$) on an Au surface, close to 300 electrons on average are emitted. Electron emission and re-neutralization continue until the hollow atom collapses upon close surface contact.

Before the projectile ion has become fully neutralized it will be accelerated towards the surface by its rapidly decreasing mirror charge, which provides an additional

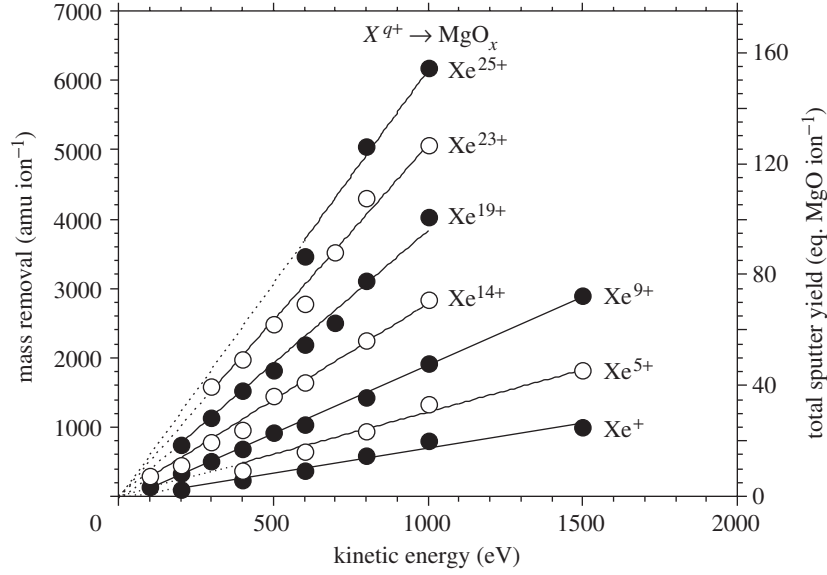


Figure 12. Measured sputter yield of MgO_x for impact of Xe^{q+} ions as a function of ion-impact energy. (Data from Hayderer *et al.* (2001b)).)

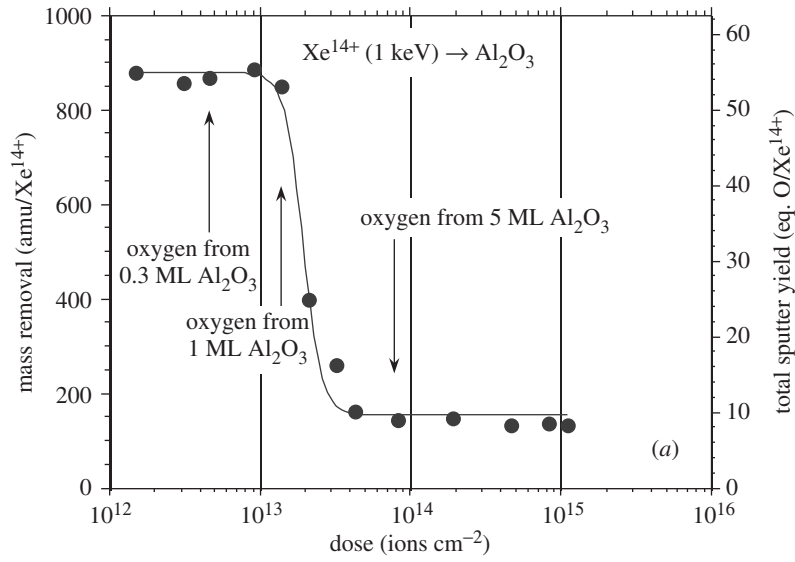


Figure 13. Mass removal due to sputtering of Al_2O_3 by Xe^{14+} ions (impact energy 1 keV) versus total ion dose. (Data from Hayderer *et al.* (2001a)). ML denotes the monolayer; the solid line is for guidance only.)

‘vertical kinetic energy’ (Burgdörfer *et al.* 1991; Arnau *et al.* 1997)

$$\Delta E_{q,\text{im}} \approx 0.25q^3/2W. \quad (5.3)$$

For our Ar^{18+} example above, $\Delta E_{q,\text{im}}$ amounts to more than 80 eV. This image charge acceleration could be demonstrated experimentally in different ways (Aumayr

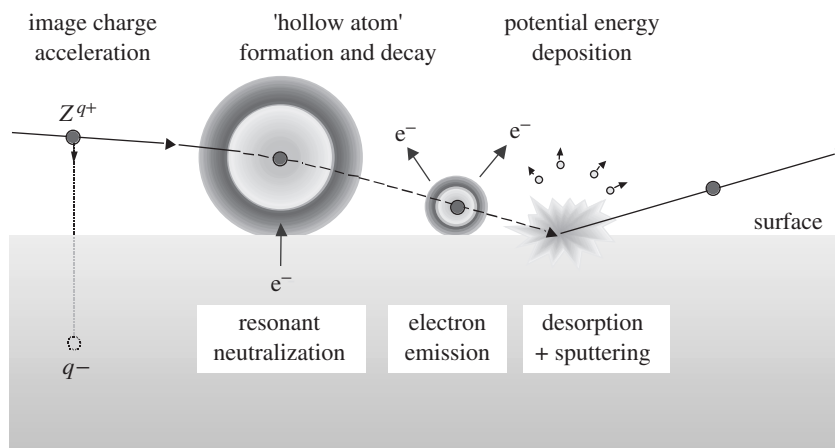


Figure 14. Scenario for impact of a slow highly charged ion on a surface (see text for further explanation).

et al. 1993; Winter *et al.* 1993; Meyer *et al.* 1995), in excellent agreement with the classical over-the-barrier-model predictions.

The projectiles become completely neutralized in front of the surface and excited states decay rapidly by autoionization to yield ample emission of low-energy electrons. However, only a fraction of the potential energy originally stored in the projectile is released above the surface, because the image charge attraction limits the interaction time available. A larger part of this potential energy will thus only be liberated in close vicinity to, or even below, the surface, when Rydberg electrons become ‘peeled off’ and more tightly bound shells (e.g. M, L, K) have become filled by Auger neutralization from the conduction band or in close collisions with target atoms (Schippers *et al.* 1993; Arnau *et al.* 1995, 1997; Stolterfoht *et al.* 1995). In this way, the potential energy of the projectile is converted into kinetic energy of the emitted electrons and electronic excitation of a small surface region. This electronic excitation consists of electron–hole pairs, ‘hot holes’ in the conduction and/or valence band of the target, and inner-shell holes of target atoms. For metal surfaces, such sudden perturbations of the electronic structure can be rapidly accommodated and the excitation energy will dissipate within the target material without inducing structural surface modification (this is the reason for the lack of dependence of the sputtering on the charge state for Au, Si and GaAs reported in §4*a*). In materials with reduced electron mobility (e.g. insulator targets), the sudden modification of the near-surface electronic structure cannot immediately be restored and may therefore induce structural surface modifications (defect formation, desorption, sputtering, etc.). This is the origin of sputtering induced by the projectile’s potential energy, i.e. potential sputtering.

Depending on the surface material and/or the charge state and impact energy of the projectiles, several models for the conversion of electronic excitation into kinetic energy of desorbed or sputtered target atoms and ions have been proposed in the past. In the following sections we briefly describe these models and compare their predictions with experimental results.

(b) Coulomb explosion

In the ‘Coulomb explosion’ (CE) model proposed by Parilis and co-workers (Parilis 1969; Bitenski *et al.* 1979; Bitenski & Parilis 1989), the neutralization of an HCI impinging on an insulator surface is assumed to cause a strong electron depletion in the near-surface region. Consequently, the mutual Coulomb repulsion of target-ion cores gives rise to the ejection of secondary ions from positively charged microscopic surface domains. Shock waves generated by this CE then ablate further target material (emission of neutral target atoms/clusters). In this way the CE model not only explains an enhanced secondary-ion emission yield but also accounts for sputtering of neutrals.

The CE model has long been favoured, most probably because of its simplicity, but, with the exception of proton sputtering from hydrogen covered surfaces (Kakutani *et al.* 1995a; Burgdörfer & Yamazaki 1996), has so far failed to provide even a semi-quantitative interpretation of the experimental data (Aumayr *et al.* 1999). Molecular dynamics (MD) simulations for CE processes in pure Si (Cheng & Gillaspay 1997) are in contradiction to experimental results with respect to the ionization degree of sputtered particles as well as their energy distribution. The main argument against the CE model is that, even in insulators, the hole lifetimes are short enough to facilitate re-neutralization before the lattice can respond (Aumayr *et al.* 1999). Some authors (Mochiji *et al.* 1996; Schenkel *et al.* 1999), however, argue that hole lifetimes might become considerably longer when many holes are generated in close vicinity. The absence of a significant number of (singly or multiply) charged secondary ions (at most a few per cent of all sputtered particles are in the ionized state (Neidhart *et al.* 1995a; Schenkel *et al.* 1998a, b, 1999)), however, points to a low ionization density even near the centre of the ion impact and makes it questionable whether conditions for CE can be achieved. Most authors nowadays agree (Schenkel *et al.* 1999) that if CE is possible at all, it will only play a role for projectile ions in very high charge states but is not relevant for ion impact with intermediate q , as presented in § 4.

(c) Sputtering by intense, ultrafast electronic excitation

This model was originally developed to describe non-thermal phase transitions of semiconductors induced by intense ultrafast electronic excitations from femtosecond lasers (Stampfli & Bennemann 1996). It considers the effect of a high density of electronic excitation on the structural stability of covalent solids like Si, GaAs and SiO₂. Destabilization of atomic bonds is induced when many valence electrons (of the order of one per atom) are promoted from bonding states in the valence band to anti-bonding states in the conduction band, causing a repulsive force between individual atoms. The critical laser fluence necessary to induce such a phase transition is 0.8 kJ m⁻² (Stampfli & Bennemann 1996) with a characteristic absorption depth of *ca.* 1 μm. This value can also be reached by slow ions in very high charge states. Therefore, this model might explain why potential sputtering of GaAs is observed for ions such as Th⁷⁰⁺ or Xe⁴⁴⁺ (Schenkel *et al.* 1998b) but not for Ar^{*q*+} ($q \leq 9$) as shown in § 4a.

(d) Defect-mediated sputtering

The ‘defect-mediated sputtering’ (DS) model considers formation of localized defects, such as ‘self-trapped excitons’ (STEs) or ‘self-trapped holes’ (STHs) in

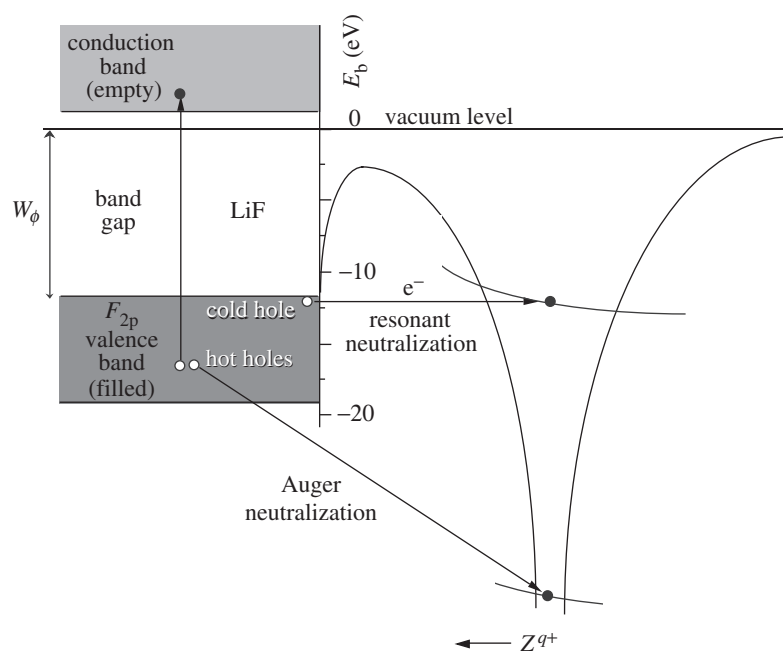


Figure 15. Electronic transitions between surface and projectile ion leading to formation of holes (via resonant neutralization) as well as electron-hole pairs (via Auger neutralization).

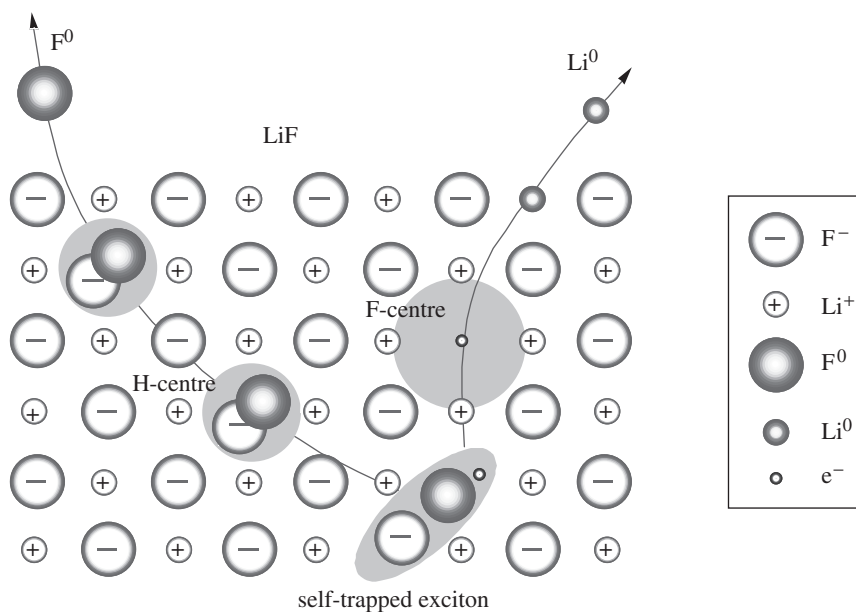


Figure 16. The potential sputtering process for LiF explained according to the DS model (see text).

response to valence-band excitations (Neidhart *et al.* 1995*b*; Sporn *et al.* 1997; Aumayr *et al.* 1999; Hayderer *et al.* 1999*a*). In certain insulator materials (alkali halides, SiO₂, Al₂O₃) electronic defects can be induced by bombardment with energetic electrons (electron stimulated desorption, or ESD) as well as ultraviolet photons (photon stimulated desorption, PSD) (Green *et al.* 1987; Walkup *et al.* 1987; Szymonski *et al.* 1992; Seifert *et al.* 1993; Szymonski 1993). As described above, the strong interaction of HCIs with any target surface causes formation of electron–hole pairs and ‘hot holes’ (i.e. holes in the ‘deeper’ part of the valence band; see figure 15).

Due to the strong electron–phonon coupling (i.e. efficient energy transfer from the electronic to the phononic system of the solid) in alkali halides and SiO₂, such an electronic excitation of the valence band becomes localized by ‘self-trapping’, i.e. STEs or STHs trapped in a self-produced lattice deformation (Williams *et al.* 1986; Williams & Song 1990), respectively (figure 16).

As in the case of ESD/PSD, decay of such STHs and/or STEs into different ‘colour centres’ (e.g. H and F centres in the case of alkali halides, or E’ centres in the case of SiO₂) leads to the desorption of neutralized anions (halide atoms, oxygen). In LiF, for example, an H centre is an F₂ molecular ion at an anion lattice site, while an F centre is an electron localized at the next or second-next anion site (Williams *et al.* 1986; Williams & Song 1990). The neutral cations created in this way are either evaporated (as in the case of heated alkali-halide samples) or can be removed by small momentum transfer from the impinging projectiles.

As an example, in figure 16, the potential sputtering process for a LiF target surface is depicted schematically. If the HCI approaches the LiF surface, holes in the F(2p) valence band will be created by resonance neutralization (RN). ‘Cold holes’ (i.e. holes localized at the Fermi edge) in the first surface layer will form V_k centres (F₂ molecular ions adjacent to two anion sites) (Williams *et al.* 1986; Williams & Song 1990), while the resulting highly excited projectiles become de-excited by Auger and autoionization processes, leading to electron emission. When the projectile penetrates the surface layer while it is still in an ionized or highly excited state, interatomic Auger neutralization (AN) and RN (figure 15) will take place and further neutralize and/or de-excite the projectile, producing more holes and electron–hole pairs. ‘Hot holes’ will be formed with higher probability because of the larger electron density in the centre of the valence band. Therefore, resulting V_k centres can trap available electrons, thus forming STEs, which at room temperature will rapidly decay into two colour centres, i.e. an H centre (F₂ molecular ion at one anion lattice site) and an F centre (electron localized at the next or second-next anion site) (Williams *et al.* 1986; Williams & Song 1990). H and F centres created in the bulk can diffuse to the surface, where the H centre will decay by emitting an F⁰ atom and the F centre may neutralize a Li⁺ cation. For electron bombardment, Li atoms created at the surface will form a metallic overlayer which eventually stops further progress of ESD or PSD at room temperature, but can be evaporated at surface temperatures above 150 °C. In contrast to ESD, even at rather low impact energy the much heavier HCI projectiles provide sufficient momentum transfer for removing single weakly (van der Waals) bound Li atoms from the LiF surface, which ensures stoichiometric desorption at low surface temperature. Within the DS model for PS it is not sufficient for a target surface to be an insulator. An enhancement of the absolute total sputter yields with increasing charge state of the primary ion

is possible only for targets with strong electron–phonon coupling, where electronic excitation can be localized by formation of STEs and/or STHs.

Experimental evidence presented for LiF, NaCl, SiO₂ and Al₂O₃ in § 4*b, c* fully supports the DS model described above. In the following we will summarize the main indications.

- (i) All these materials (LiF, NaCl, SiO₂ and Al₂O₃) are known to exhibit strong electron–phonon coupling and STH or STE formation (Williams *et al.* 1986; Williams & Song 1990).
- (ii) For all other targets (Au, Si, GaAs and MgO) no STH or STE formation is known. With the exception of MgO (which will be discussed separately in § 5*e*) these targets only show kinetically induced sputtering up to the highest applied ion-charge states.
- (iii) The electronic defects in the surface (e.g. the number of electron–hole pairs and holes created) should be roughly proportional to the potential energy carried by the projectile into the surface. In the case of DS the number of STHs and STEs and, consequently, the number of sputtered particles, should therefore increase nearly linearly with the potential energy, as has been observed in experiment (see, for example, figure 8*a*).
- (iv) At very low impact energy on SiO₂ and Al₂O₃ the effect of potential sputtering was found to decrease with increasing ion dose. According to the DS model, the cations are removed by evaporation (alkali halides) or by momentum transfer from the impinging projectile to the now weakly bound (neutralized) cation. In SiO₂ and Al₂O₃ the removal of the cations is only possible by the latter mechanism (the main difference between alkali halides and oxides). Therefore, at very low impact energy only oxygen is sputtered and the surface becomes enriched in Si or Al. Consequently, the potential sputtering effect decreases with increasing ion dose. In the case of ESD from LiF, a similar mechanism causes formation of a metallic Li overlayer at low target temperatures (Szymonski *et al.* 1992).
- (v) The threshold for potential sputtering of LiF found in experiments with various singly and doubly charged ions (figure 8*b*) is the most convincing evidence for the DS model. For alkali halides, resonant capture of an electron from a surface site can generate an STH. According to the simple picture provided in figure 15, the energy required for this process is of the order of 10–12 eV. More refined calculations on the basis of a simple two-state curve-crossing analysis between the perturbed valence band of LiF and the perturbed ground state of the projectile show that the experimentally observed threshold at 10 eV (figure 8*b*) coincides exactly with the energy necessary to produce a cold hole (STH) in the valence band of LiF via resonant electron capture (Hayderer *et al.* 1999*a*). Moreover, above a potential energy of 20 eV, Auger capture (figure 15) becomes possible, which leads to the formation of an electron–hole pair localizing as an STE. Its decay into colour centres leads to the formation and emission of neutral Li and F at the surface. This expected increase in the sputter yield has been marked in figure 8*b* but is, however, too small for unambiguous identification in our experimental data.

When changing from singly to doubly charged projectiles the stepwise neutralization leads to the formation of at least one additional STH and therefore to a considerable increase in the sputtering yield. Such an increase is indeed observed above 30 eV potential energy (figure 8*b*), if at least 10 eV potential energy remains for the second neutralization step ($X^+ \rightarrow X^0$). This is the case for all doubly charged ions with the exception of Na^{2+} . Although Na^{2+} projectiles carry more than 50 eV recombination energy, almost all of this energy is used for the first neutralization step ($\text{Na}^{2+} \rightarrow \text{Na}^+$) and the remaining potential energy of 5.1 eV is below the threshold for potential sputtering, which explains the exceptionally small sputter yield for Na^{2+} .

(*e*) *Kinetically assisted potential sputtering*

From the above arguments we have to conclude that trapping of electronic defects due to strong electron–phonon coupling is essential in defect-mediating potential sputtering. Self-trapping is known to occur in alkali halides, SiO_2 and Al_2O_3 but not in highly ionic oxides like MgO_x . Consequently, we did not expect PS for MgO_x , and first preliminary experiments with Ar^{q+} ($q \leq 8$) on MgO did not indicate PS (Varga *et al.* 1997). It came as a big surprise that a strong charge state effect was present (see figure 12), when we bombarded MgO_x with multiply charged Xe ions (charge states up to $q = 25$) (Hayderer *et al.* 2001*b*). The unusual behaviour of the measured total sputtering yields for MgO_x with projectile impact velocity shown in figure 12, however, led us to the conclusion that we had encountered a new form of PS. Although the potential energy greatly enhances the total sputtering yield Y (yield is proportional to the potential energy W_{pot}), it does not seem to be sufficient to induce PS on its own. Extrapolation of Y to zero kinetic energy for all charge states is consistent with zero sputtering yield. Conspicuously large sputtering yields are achieved only in combination with projectile kinetic energy. This new form of potential sputtering obviously requires the electronic excitation of the target material (believed to be the precursor of the usual PS process) and the formation of a collision cascade within the target (and therefore a finite projectile kinetic energy) simultaneously in order to initiate the sputtering process. This new mechanism was termed ‘kinetically assisted potential sputtering’ (KAPS) (Hayderer *et al.* 2001*b*).

In the following we will sketch a model for this new mechanism, which combines our knowledge about the neutralization of slow HCIs upon surface impact with that for radiation-induced processes in non-metallic solids (Itoh 1998). According to the DS model described above, a localization of the electronic surface excitation by the HCI is required in order to effectively transfer the electronic energy into the kinetic energy of the atomic and molecular particles to be desorbed. One (important) mechanism for pinning of the electronic excitations is trapping at lattice defects. In insulating solids with strong electron–phonon coupling a strong lattice distortion gives rise to self-trapping (see § 5*d*). In other materials a localization of electronic excitation energy can only occur at already present defects (Itoh 1998) created by other processes or at interfaces. It is therefore plausible to assume that the kinetic energy of the projectile via a collision cascade may be responsible for generating the ‘seed’ for trapping of electronic excitations. At the impact of an Xe projectile of several 100 eV, elastic collision processes—even below the knock-on threshold for sputtering—can lead to a strong temporary displacement of the lattice atoms and therefore provides sites for

localization of electronic excitation energy. This scenario can be translated into a set of coupled rate equations for the sputtering yield Y valid for any insulating crystal (Hayderer *et al.* 2001b),

$$\frac{dY}{dt} = c_P N_{ST} + c_{KP} N_{LD} N_{ED}, \quad (5.4)$$

where c_P describes the conversion rate of a self-trapped electronic defect into desorption of surface particles (i.e. ‘conventional’ potential sputtering) and c_{KP} is the corresponding conversion rate of a pair of electronic and kinetically induced lattice defects. Analogous rate equations for N_{ST} (the number of self-trapped electronic defects), N_{LD} (the number of lattice defects) and N_{ED} (the number of electronic defects) close the system. In the case of MgO_x , c_P is zero, signifying the absence of self-trapping, while, for target materials that feature self-trapped electronic defects (LiF, NaCl, SiO_2 and Al_2O_3), a non-zero value of c_P is responsible for the measured sputtering yield at zero kinetic energy (cf. figures 6, 7, 10 and 11). Since SRIM-2000 simulations (Ziegler *et al.* 1985) indicate that N_{LD} is proportional to the kinetic energy of the projectile, the second term in equation (5.4) gives rise to a sputtering yield Y which increases linearly with kinetic energy and where the slope is a function of the charge state q , due to the increased number of electronic defects N_{ED} for projectiles with higher q .

Projectiles with sufficient kinetic energy produce a large number of lattice defects N_{LD} along their trajectory in the target, which are serving as possible trapping sites. At these sites the large number of electronic defects produced by highly charged Xe^{q+} may get localized, resulting in the surprisingly large sputtering yields observed in our experiment. This kinetically assisted potential sputtering (KAPS) (the second term in equation (5.4)) should, however, also be observable for target materials where self-trapping is possible (cases with $c_P \neq 0$). And indeed, a closer inspection of figures 6, 10 and 11 reveals that in the case of LiF, SiO_2 and Al_2O_3 , the sputtering yield also increases linearly for increasing kinetic energy, with the slope being a steep (increasing) function of the charge state q . This behaviour cannot be explained by conventional kinetic sputtering and has not been recognized in the past, since it is over-shadowed by the comparably much stronger contribution from desorption due to self-trapped defects (the first term in equation (5.4)). The identification of a so-far-unrecognized kinetically assisted potential sputtering process is therefore *not* based on the results for MgO_x alone (although these data did provide the first clue that a considerably more complex behaviour was at hand than was believed earlier). The KAPS mechanism seems to be present in a larger variety of target materials and might also provide an explanation for several projectile charge-state-dependent sputtering and secondary-ion-emission phenomena observed at considerably higher kinetic energies (see Schenkel *et al.* 1999 and references therein).

6. Possible applications of potential sputtering

The possibility of exploiting the huge amount of potential energy stored in highly charged ions for nanofabrication, for example, ‘writing’ on a surface, has captured the imagination of researchers for some time. A broad spectrum of applications have been envisioned for, from information storage via materials processing to biotechnology.

While nanostructures produced by kinetic sputtering with, and implantation of, *fast* ions are subject to unwanted radiation damage, potential sputtering by HCIs promises a much more gentle nanostructuring tool, since

- (i) their kinetic energy is small, so they will interact only with the first few surface layers, without penetrating deeper into the target bulk;
- (ii) they interact with the surface mainly through their potential energy, which can be tuned by varying the ion charge;
- (iii) the potential energy causes primarily electronic excitation which leads to bond breaking and lattice defect production via electron–phonon coupling rather than violent momentum transfer in kinetic collision cascades;
- (iv) the interaction of slow MCI with surfaces is highly material selective, i.e. large differences between (semi-) conducting and insulating target materials are observed.

The KAPS mechanism considerably expands the opportunities to modify surfaces by beams of slow, highly charged ions.

Production of nano-defects due to HCI impact on atomically clean single crystal surfaces has already been studied by using atomic force microscopy (AFM) and scanning tunnelling microscopy (STM) (Gebeshuber *et al.* 2003).

As a next step we intend to use beams of slow multi-charged ions to produce nanometre-sized surface modifications on silicon substrates. This will be achieved by bombarding hydrogen-terminated silicon monocrystals in an UHV with low fluxes of slow HCIs. At the HCI-impact site (with 1 nm radius) we expect the hydrogen atoms to be removed by the interaction of the MCI with the surface. By introducing oxygen gas of sufficient partial pressure, the now open silicon bonds will react with the O₂ molecules, in this way producing ultra-shallow silicon oxide nanodots (Borsoni *et al.* 2002). We intend to study the formation of these nanodots and to optimize the conditions by using (non-contact) atomic AFM and STM, as well as high-resolution-scanning Auger spectroscopy. Later on we will investigate whether carbon nanotubes or other multi-molecular structures can be preferentially grown on such small silicon oxide nanodots (Wei *et al.* 2002).

After a decade of primarily basic investigations of the underlying mechanisms, the first promising applications of multi-charged ions for engineering the topmost layers of insulating surfaces are finally emerging.

This work has been supported by Fonds zur Förderung der wissenschaftlichen Forschung, Wirtschaftskammer Wien and was carried out within Association EURATOM-ÖAW. Fruitful collaborations with J. Burgdörfer, C. Lemell, M. Schmid and P. Varga (TU Wien) and N. Stolterfoht (HMI Berlin), and the participation of T. Neidhart, M. Sporn, D. Niemann, M. Grether, G. Hayderer and S. Cernusca in some of the experiments are gratefully acknowledged.

References

Arnau, A., Zeijlmans van Emmichoven, P. A., Juaristi, J. I. & Zaremba, E. 1995 Nonlinear screening effects in the interaction of slow multi-charged ions with metal-surfaces. *Nucl. Instrum. Meth. Phys. Res. B* **100**, 279–283.

Phil. Trans. R. Soc. Lond. A (2004)

- Arnau, A. (and 13 others) 1997 Interaction of slow multi-charged ions with solid surfaces. *Surf. Sci. Rep.* **27**, 117–239.
- Arnoldbik, W. M., Tomozeiu, N. & Habraken, F. H. P. M. 2003 Electronic sputtering of thin SiO₂ films by MeV heavy ions. *Nucl. Instrum. Meth. Phys. Res. B* **203**, 151–157.
- Aumayr, F. 1995 Interaction of highly charged ions with metal and insulator surfaces. In *The physics of electronic and atomic collisions* (ed. L. J. Dubé, J. B. A. Mitchell, J. W. McConkey & C. E. Brion), vol. 360, p. 31. New York: AIP Press.
- Aumayr, F., Kurz, H., Schneider, D., Briere, M. A., McDonald, J. W., Cunningham, C. E. & Winter, H. P. 1993 Emission of electrons from a clean gold surface-induced by slow, very highly charged ions at the image charge acceleration limit. *Phys. Rev. Lett.* **71**, 1943–1946.
- Aumayr, F., Burgdörfer, J., Varga, P. & Winter, H. P. 1999 Sputtering of insulator surfaces by slow highly charged ions: Coulomb explosion or defect mediated desorption? *Comm. Atom. Mol. Phys.* **34**, 201–209.
- Bitenskii, I. S., Murakhmetov, M. N. & Parilis, E. S. 1979 Atomization of non-metals by multi-charge ions of average energies, using the Coulomb burst. *Sov. Phys. Tech. Phys.* **24**, 618–621.
- Bitenskii, I., Parilis, E., Della-Negra, S. & LeBeyec, Y. 1992 New method for measuring sputtering in region near threshold. *Nucl. Instrum. Meth. Phys. Res. B* **72**, 380–386.
- Bitensky, I. S. & Parilis, E. S. 1989 The sputtering of non-metals under slow multiply charged ions. *J. Phys. Paris C* **2**, 227–230.
- Borsoni, G. (and 11 others) 2002 Ultrathin SiO₂ layers formation by ultraslow single- and multi-charged ions. *Solid State Electron.* **46**, 1855–1862.
- Burgdörfer, J. 1993 Atomic collisions with surfaces. In *Fundamental processes and applications of atoms and ions* (ed. C. D. Lin). Singapore: World Scientific.
- Burgdörfer, J. & Yamazaki, Y. 1996 Above-surface potential sputtering of protons by highly charged ions. *Phys. Rev. A* **54**, 4140–4144.
- Burgdörfer, J., Lerner, P. & Meyer, F. W. 1991 Above-surface neutralization of highly charged ions: the classical over-the-barrier model. *Phys. Rev. A* **44**, 5674–5685.
- Cheng, H. P. & Gillaspay, J. D. 1997 Nanoscale modification of silicon surfaces via Coulomb explosion. *Phys. Rev. B* **55**, 2628–2636.
- Della-Negra, S., Depauw, J., Joret, H., Le-Beyec, V. & Schweikert, E. A. 1988 Secondary ion emission induced by multi-charged 18-keV ion-bombardment of solid targets. *Phys. Rev. Lett.* **60**, 948–951.
- de Zwart, S. T., Fried, T., Boerma, D. O., Hoekstra, R., Drentje, A. G. & Boers, A. L. 1986 Sputtering of silicon by multiply charged ions. *Surf. Sci.* **177**, L939–L946.
- Eccles, A. J., van den Berg, J. A., Brown, A. & Vickerman, C. 1986 Evidence of a charge induced contribution to the sputtering yield of insulating and semiconducting materials. *Appl. Phys. Lett.* **49**, 188–190.
- Ellegard, O., Schou, J., Sørensen, H. & Børjesen, P. 1986 Electronic sputtering of solid nitrogen and oxygen by keV electrons. *Surf. Sci.* **167**, 474–492.
- Gebeshuber, I. C., Cernusca, S., Aumayr, F. & Winter, H. P. 2003 AFM search for slow MCI-produced nanodefects on atomically clean monocrystalline surfaces. *Nucl. Instrum. Meth. Phys. Res. B* **205**, 751–757.
- Gnaser, H. 1999 *Low-energy ion irradiation of solid surfaces*. Springer.
- Green, T. A., Loubriel, G. M., Richards, P. M., Tolk, N. H. & Haglund, R. F. 1987 Time-dependence of desorbed ground-state lithium atoms following pulsed-electron-beam irradiation of lithium-fluoride. *Phys. Rev. B* **35**, 781–787.
- Hägg, L., Reinhold, C. O. & Burgdörfer, J. 1997 Above-surface neutralization of slow highly charged ions in front of ionic crystals. *Phys. Rev. A* **55**, 2097–2108.
- Hayderer, G., Schmid, M., Varga, P., Winter, H., Aumayr, F., Wirtz, L., Lemell, C., Burgdörfer, J., Hägg, L. & Reinhold, C. O. 1999a Threshold for potential sputtering of LiF. *Phys. Rev. Lett.* **83**, 3948–3951.

- Hayderer, G., Schmid, M., Varga, P., Winter, H. P. & Aumayr, F. 1999b A highly sensitive quartz-crystal microbalance for sputtering investigations in slow ion-surface collisions. *Rev. Scient. Instrum.* **70**, 3696–3700.
- Hayderer, G., Cernusca, S., Hoffmann, V., Niemann, D., Stolterfoht, N., Schmid, M., Varga, P., Winter, H. & Aumayr, F. 2001a Sputtering of Au and Al₂O₃ surfaces by slow highly charged ions. *Nucl. Instrum. Meth. Phys. Res. B* **182**, 143–147.
- Hayderer, G. (and 11 others) 2001b Kinetically assisted potential sputtering of insulators by highly charged ions. *Phys. Rev. Lett.* **86**, 3530–3533.
- Itoh, N. 1998 Subthreshold radiation-induced processes in the bulk and on surfaces and interfaces of solids. *Nucl. Instrum. Meth. Phys. Res. B* **135**, 175–183.
- Kakutani, N., Azuma, T., Yamazaki, Y., Komaki, K. & Kuroki, K. 1995a Strong charge-state dependence of H⁺ and H₂⁺ sputtering induced by slow highly charged ions. *Nucl. Instrum. Meth. Phys. Res. B* **96**, 541–544.
- Kakutani, N., Azuma, T., Yamazaki, Y., Komaki, K. & Kuroki, K. 1995b Potential sputtering of protons from a surface under slow highly charged ion-bombardment. *Jpn. J. Appl. Phys.* **34**, 580–583.
- McKeown, C. 1961 New method for measuring sputtering in region near threshold. *Rev. Scient. Instrum.* **32**, 133–136.
- Meyer, F. W., Folkerts, L., Folkerts, H. O. & Schippers, S. 1995 Projectile image acceleration, neutralization and electron-emission during grazing interactions of multi-charged ions with Au (110). *Nucl. Instrum. Meth. Phys. Res. B* **98**, 441–444.
- Mochiji, K., Itabashi, N., Yamamoto, S., Ichiai, I. & Okuno, K. 1994 Surface-reaction induced by multiply charged ions. *Jpn. J. Appl. Phys.* **33**, 7108–7111.
- Mochiji, K., Itabashi, N., Yamamoto, S., Shimizu, S., Ohtani, S., Kato, Y., Tanuma, H., Okuno, K. & Kobayashi, N. 1996 Desorption induced by electronic potential energy of multiply charged ions. *Surf. Sci.* **358**, 673–677.
- Morgenstern, R. & Das, J. 1994 The interaction of highly charged ions with surfaces. *Europhys. News* **25**, 3–6.
- Morozov, S. N., Gurich, D. D. & Arifov, T. U. 1979 Ion and electron-emission of LiF, NaCl and Si mono-crystals under the influence of multicharged ions of various elements. *Izv. Akad. Nauk SSSR* **43**, 612–618.
- Murty, M. V. R. 2002 Sputtering: the material erosion tool. *Surf. Sci.* **500**, 523–544.
- Neidhart, T., Toth, Z., Hochhold, M., Schmid, M. & Varga, P. 1994 Total sputter yield of LiF induced by hyperthermal ions measured by a quartz microbalance. *Nucl. Instrum. Meth. Phys. Res. B* **90**, 496–500.
- Neidhart, T., Pichler, F., Aumayr, F., Winter, H. P., Schmid, M. & Varga, P. 1995a Secondary-ion emission from lithium-fluoride under impact of slow multi-charged ions. *Nucl. Instrum. Meth. Phys. Res. B* **98**, 465–468.
- Neidhart, T., Pichler, F., Aumayr, F., Winter, H. P., Schmid, M. & Varga, P. 1995b Potential sputtering of lithium-fluoride by slow multi-charged ions. *Phys. Rev. Lett.* **74**, 5280–5283.
- Neidhart, T., Pichler, F., Aumayr, F., Winter, H. P., Schmid, M. & Varga, P. 1995c Secondary-ion emission from lithium-fluoride under impact of slow multicharged ions. *Nucl. Instrum. Meth. Phys. Res. B* **98**, 465–468.
- Parilis, E. 1969 A mechanism for sputtering of non-metals by slow multiply charged ions. In *Proc. Int. Conf. Phenomena in Ionized Gases*, pp. 324–327. Bucharest: Editura Academia Republicii Socialiste Romania.
- Parks, D. C., Stöckli, M. P., Bell, E. W., Ratliff, L. P., Schmieder, R. W., Serpa, F. G. & Gillaspay, J. D. 1998 Non-kinetic damage on insulating materials by highly charged ion bombardment. *Nucl. Instrum. Meth. Phys. Res. B* **134**, 46–52.
- Radzhabov, S. S. & Rakhimov, R. R. 1985 Sputtering of alkali-haloid crystals under the multi-charged ion-bombardment. *Izv. Akad. Nauk SSSR* **49**, 1812–1815.

- Radzhabov, S. S., Rakhimov, R. R. & Abdusalumov, P. 1976 Secondary-emission of alkali-halide crystals by bombardment with $\text{Ar}^+ - \text{Ar}^{5+}$ and $\text{Kr}^+ - \text{Kr}^{5+}$ multi-charge ions. *Izv. Akad. Nauk SSSR* **40**, 2543–2547.
- Schenkel, T., Briere, M. A., Schmidt-Böcking, H., Bethge, K. & Schneider, D. H. 1997 Electronic sputtering of thin conductors by neutralization of slow highly charged ions. *Phys. Rev. Lett.* **78**, 2481–2484.
- Schenkel, T., Barnes, A. V., Hamza, A. V., Schneider, D. H., Banks, J. C. & Doyle, B. L. 1998a Synergy of electronic excitations and elastic collision spikes in sputtering of heavy metal oxides. *Phys. Rev. Lett.* **80**, 4325–4328.
- Schenkel, T., Hamza, A. V., Barnes, A. V., Schneider, D. H., Banks, J. C. & Doyle, B. L. 1998b Ablation of GaAs by intense, ultrafast electronic excitation from highly charged ions. *Phys. Rev. Lett.* **81**, 2590–2593.
- Schenkel, T., Hamza, A. V., Barnes, A. V. & Schneider, D. H. 1999 Interaction of slow, very highly charged ions with surfaces. *Prog. Surf. Sci.* **61**, 23–84.
- Schippers, S., Hustedt, S., Heiland, W., Köhrbrück, R., Bleck-Neuhaus, J., Kemmler, J., Lecler, D. & Stolterfoht, N. 1993 Deexcitation of hollow atoms—autoionization of multiply excited N, O and Ne atoms at a Pt (110) surface. *Nucl. Instrum. Meth. Phys. Res. B* **78**, 106–112.
- Schiwietz, G., Luderer, E., Xiao, G. & Grande, P. L. 2001 Energy dissipation of fast heavy ions in matter. *Nucl. Instrum. Meth. Phys. Res. B* **175–177**, 1–11.
- Schneider, D. H. & Briere, M. A. 1996 Investigations of the interactions of highest charge state ions with surfaces. *Physica Scr.* **53**, 228–242.
- Schneider, D. H., Briere, M. A., McDonald, J. & Biersack, J. 1993 Ion–surface interaction studies with 1–3 keV/AMU ions up to Th^{80+} . *Rad. Eff. Def. Solids* **127**, 113–136.
- Seifert, N., Liu, D., Barnes, A., Albridge, R., Yan, Q., Tolck, N., Husinsky, W. & Betz, G. 1993 Simultaneous laser-induced fluorescence and quadrupole-mass-spectroscopy studies of electron-stimulated desorption of ground-state lithium atoms from lithium-fluoride crystals. *Phys. Rev. B* **47**, 7653.
- Sigmund, P. (ed.) 1993 *Proc. Fundamental Processes in Sputtering of Atoms and Molecules (SPUT 92)*, Copenhagen. *Mat.-Fys. Medd. K. Dan. Vidensk. Selsk.*
- Sporn, M., Libiseller, G., Neidhart, T., Schmid, M., Aumayr, F., Winter, H. P., Varga, P., Grether, M. & Stolterfoht, N. 1997 Potential sputtering of clean SiO_2 by slow highly charged ions. *Phys. Rev. Lett.* **79**, 945–948.
- Stampfli, P. & Bennemann, K. H. 1996 Theory for the laser-induced femtosecond phase transition of silicon and GaAs. *Appl. Phys. A* **60**, 191–196.
- Stolterfoht, N., Köhrbrück, R., Grether, M., Spieler, A., Arnau, A., Page, R., Saal, A., Thomaschewski, J. & Bleck-Neuhaus, J. 1995 Models for L-shell filling of slow hollow atoms moving below a surface. *Nucl. Instrum. Meth. Phys. Res. B* **99**, 4.
- Szymonski, M. 1993 Electronic sputtering of alkali halides. *Mat.-Fys. Medd. K. Dan. Vidensk. Selsk.* **43**, 495–526.
- Szymonski, M., Poradisz, A., Czuba, P., Kolodziej, J., Piatkowski, P., Fine, J., Tanovic, L. & Tanovic, N. 1992 Electron-stimulated desorption of neutral species from (100) KCl surfaces. *Surf. Sci.* **260**, 295–303.
- Varga, P., Neidhart, T., Sporn, M., Libiseller, G., Schmid, M., Aumayr, F. & Winter, H. P. 1997 Sputter yields of insulators bombarded with hyperthermal multiply charged ions. *Physica Scr.* **T73**, 307–310.
- Walkup, R. E., Avouris, P. & Ghosh, A. 1987 Positive-ion production by electron-bombardment of alkali-halides. *Phys. Rev. B* **36**, 4577–4580.
- Wei, B. Q., Vajtai, R., Jung, Y., Ward, J., Zhang, R., Ramanath, G. & Ajayan, P. M. 2002 Organized assembly of carbon nanotubes: cunning refinements help to customize the architecture of nanotube structures. *Nature* **416**, 495–496.

- Williams, R. T. & Song, K. S. 1990 The self-trapped exciton. *J. Phys. Chem.* **51**, 679–716.
- Williams, R. T., Song, K. S., Faust, W. L. & Leung, C. H. 1986 Off-center self-trapped excitons and creation of lattice-defects in alkali-halide crystals. *Phys. Rev. B* **33**, 7232–7240.
- Winter, H. 2000 Scattering of atoms and ions from insulator surfaces. *Prog. Surf. Sci.* **63**, 177–247.
- Winter, H. P. & Aumayr, F. 1999 Hollow atoms. *J. Phys. B* **32**, R39–R65.
- Winter, H. P. & Aumayr, F. 2001 Interaction of slow HCl with solid surfaces: what do we know, what should we know? *Physica Scr.* **T92**, 15–21.
- Winter, H. P. & Aumayr, F. 2002 Slow multi-charged ions hitting a solid surface: from hollow atoms to novel applications. *Europhys. News* **33**, 215–217.
- Winter, H., Auth, C., Schuch, R. & Beebe, E. 1993 Image acceleration of highly charged xenon ions in front of a metal-surface. *Phys. Rev. Lett.* **71**, 1939–1942.
- Ziegler, J. F., Biersack, J. P. & Littmark, U. 1985 *The stopping and range of ions in matter*. New York: Pergamon.